A Radio Halo Found in the Hottest Known Cluster of Galaxies 1E0658-56

H. Liang

Physics Department, University of Bristol, Tyndall Avenue, Bristol, BS8 1TL, UK

Abstract. We report the detection of a diffuse radio halo source in the hottest known cluster of galaxies 1E0658-56 (RXJ0658-5557). The radio halo has a morphology similar to the X-ray emission from the hot intracluster medium. The detection of such a strong radio halo in such a hot cluster is further evidence to the link between X-ray temperature and cluster-wide radio halos. We describe a new model for the origin of cluster-wide radio halo sources involving a direct connection between the X-ray emitting thermal particles and the radio emitting relativistic particles.

1. Introduction

Diffuse cluster radio sources are found in a few X-ray luminous clusters of galaxies. They are extended (~ 1 Mpc), have low surface brightness and steep spectra ($\alpha < -1$), which cannot be identified with any one individual galaxy but rather with the whole cluster. Diffuse cluster radio sources are generally separated into 2 classes: halos and relics, where halos are centred on the X-ray emission (e.g. Coma-C is a proto-type radio halo source; Giovannini et al. 1993) whereas relics are peripheral and exhibit stronger polarisation than halos (e.g. A3667 has a large relic; Röttgering et al. 1997). In this talk, we will concentrate on halos.

Until recently, systematic surveys for radio halo sources have found few examples and the total number of known halos was ~ 5 (Feretti & Giovannini 1996). Radio halo sources are thus considered to be rare and owing to their small number, remain a poorly understood class of radio sources even though the first example, Coma-C, was discovered over 20 years ago. The spectra and some signs of polarisation indicate that halo radio emission is dominantly by the synchrotron process. However, the formation of radio halos remains a puzzle. The major questions involved are the origin of the magnetic field and the relativistic particles, and why radio halos occurs in some clusters and not in others.

A number of models have been proposed to explain the formation of radio halos (e.g. Jaffe 1977; Dennison 1980; Roland 1981). Most of these early models suggest that ultra-relativistic electrons originate either as relativistic electrons from cluster radio sources and reaccelerated by in-situ Fermi processes or turbulent galactic wakes, or as secondary electrons produced by the interaction between relativistic protons (again from cluster radio galaxies) and thermal protons. However, the energetics involved are problematic and the models could not always fit the observations. Harris et al. (1980) first suggested that radio halos are formed in cluster mergers where the merging process creates the shocks and turbulence necessary for the magnetic field amplification and high energy particle acceleration. More recently, Tribble (1993) showed that the energetics involved in a merger is more than enough to power a radio halo. The halos thus produced are transient which explains why they are rare.

In this talk, we will describe the properties of the radio halo found in one of the hottest known clusters 1E0658-56, and suggest a new model on the origins of cluster halos based on the radio and X-ray properties of all confirmed halos. Section 2 describes the radio halo found in 1E0658-56; Section 3 discusses the model. Throughout the talk we will use $H_0 = 50$ km s$^-$ Mpc^{-1}, $q_0 = 0.5$ and $\Lambda_0 = 0$.

2. A Radio Halo in 1E0658-56

Here we report the serendipitous detection of a strong radio halo source in 1E0658-56. The cluster was originally found in the Einstein slew survey (Tucker et al. 1995), and subsequent optical observations confirmed it to be a rich cluster at $z \sim 0.296$ (Tucker et al. 1998). It was selected as a candidate in the SEST campaign for the detection of the Sunyaev-Zel'dovich effect (SZ effect; Andreani et al. 1999). The cluster has high X-ray luminosity and temperature. Recent ASCA results have shown it to be one of the hottest clusters known (Tucker et al. 1998). The SEST observations show a $\sim 4\sigma$ detection of the SZ effect at 1.2mm (~ 150 GHz) and a $\sim 3\sigma$ detection at 2mm (~ 250 GHz) (Andreani et al. 1999). Subsequently, we obtained data on the ATCA at 8.8 GHz to confirm the SEST detection of the SZ effect. The ATCA observations were conducted using the special 210m array which proved to be an ex-

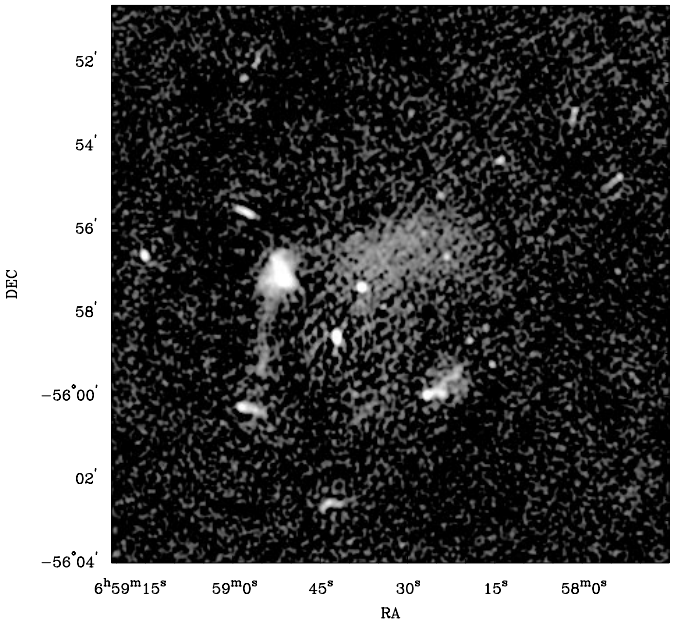

Fig. 1. A 1.3 GHz ATCA image towards the cluster 1E0658-56 at a resolution of $\sim 6''$. The noise level in the image was $\sim 44\mu$Jy/beam.

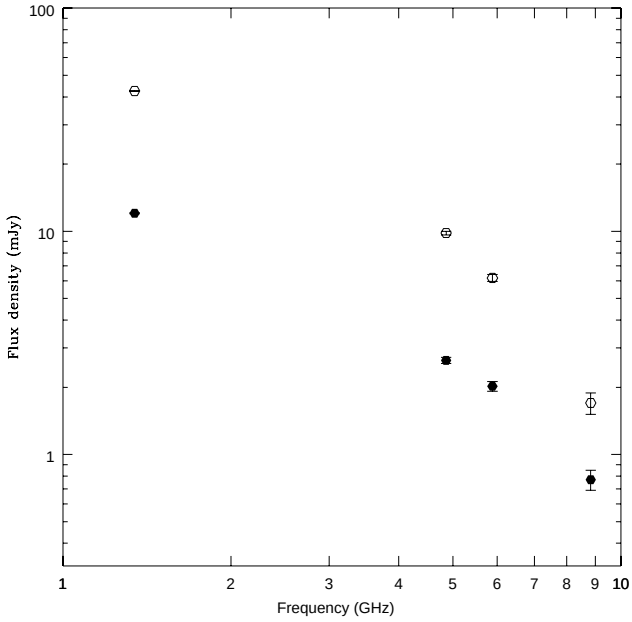

Fig. 2. Radio spectra of the cluster halo in 1E0658-56. The filled dots give the total flux within a central region ~ 210 kpc in radius, whereas the open dots corresponds to the outer regions, between radii of ~ 210 kpc and 500 kpc. The 8.8 GHz data points have not been corrected for the SZ effect.

cellent configuration for detecting low surface brightness diffuse emissions. The 4.9 GHz and 8.8 GHz observations show complex radio source structures, including at least two extended, diffuse sources and an unusual strongly polarised ($\sim 60\%$ at 8.8 GHz) steep spectrum ($\alpha \sim -1.9$) source (Liang et al. 1999). The diffuse radio sources make the detection of the SZ effect difficult since the SZ effect is also extended and the straightforward point source subtraction technique fails. However, since the radio sources in the cluster are interesting in their own right, we obtained further ATCA time to image the sources at 1.3 and 2.4 GHz bands with a 6km and two 750m arrays.

2.1. Radio Observations

The cluster was observed at the ATCA at 1.3, 2.4, 4.9, 5.9 and 8.8 GHz in several antenna configurations, so that similar uv coverage was obtained at all frequencies. The ATCA has 5 antennas on a continuous rail-track over 3 km and a 6th antenna 6km away; it enables simultaneous observations in two frequency bands each of bandwidth 128 MHz divided into 32 frequency channels. The halo was clearly detected in all frequencies. The 2.4 GHz data were heavily affected by interference and will not be considered further. A 1.3 GHz image of the cluster field is shown in Fig. 1, where we see the halo source at the cluster centre, a relic source to the east and a number of tail sources on the periphery. A radio contour image at 1.3 GHz of the halo, with embedded point sources subtracted, is shown in Fig. 3.

To obtain the spectral indices of the halo, we took data from approximately the inner uv-plane (baselines $< 3600\lambda$; λ being the wavelength) for each available frequency. The observations were planned such that roughly the same region in the uv-plane was sampled at the various frequencies. The data were tapered such that the resultant beam size was $\sim 60''$ at each frequency. To form a spectrum, the same area was used to integrate the flux at each frequency. This area was selected to include only regions of obvious emissions at all frequencies. The results are shown in Fig. 2. The spectral index of the central part of the halo is ~ -1.18 between 1.3 and 4.9 GHz, and ~ -1.40 between 4.9 and 5.9 GHz indicating possible spectral steepening at high frequencies. The data points in Fig. 2 have not been corrected for the SZ effect. The SZ effect is expected to be strongest at 8.8 GHz contributing ~ -0.5mJy in the central region, thus the true spectra would be less steep at 8.8 GHz than what we see in the plot.

2.2. X-ray Properties

The cluster was observed for 25 ksec by ASCA in May 1996. Tucker et al. (1998) analysed the ASCA GIS and SIS data as well as the ROSAT HRI data and found the cluster to have a best fit temperature of $kT_x \sim 17.4 \pm 2.5$ keV and a bolometric luminosity of $L_{bol} \sim (1.4 \pm 0.3) \times 10^{46}$ ergs s^{-1}.

Since then, some PSPC data have become publicly available and it is known that the SIS data below 1 keV suffered from inaccurate calibrations, thus we re-

estimate the cluster temperature by simultaneously fitting the ASCA GIS and ROSAT PSPC data. The GIS and PSPC data complement each other, since the GIS is more sensitive to the cluster temperature and the PSPC is more sensitive to the soft X-ray absorption.

We followed the standard ASCA procedure for screening the GIS2 and GIS3 data as set out in "The ABC guide to ASCA data reduction". The spectra were extracted from a circular region of radius 7.25′ centred on the cluster, after the subtraction of a local background, extracted from the same frame in areas where there are no obvious emission. The spectra were regrouped to a minimum of 50 counts per bin. The XSPEC package was used to fit a Raymond-Smith spectrum (Raymond & Smith 1977) with photoelectric absorption (Morrison & McCammon 1983) to the GIS spectra between 0.8 keV and 10 keV, leaving temperature, abundance, absorption (parametrised by N_H) and the normalisation as free parameters. The best fit temperature was $kT_x \sim 15.6^{+3.1}_{-2.3}$ keV.

We retrieved 4.7 ksec PSPC data observed in Feb. 1997 from the ROSAT archive. A spectrum of the X-ray emission from the cluster gas was extracted from the central $5'$ radius after the subtraction of discrete source and background contributions. The background was estimated from an annulus centred on the cluster between a radius of $8'$ to $10'$.

A combined fit of a Raymond-Smith spectrum to the GIS and PSPC spectra gave the best fit as follows: $kT_x = 14.5^{+2.0}_{-1.7}$ keV, $N_H = (4.1 \pm 0.5) \times 10^{20}$ cm^{-2}, abundance $= 0.48 \pm 0.24$ (see Fig. 4; errors correspond to 90% confidence limit). Thus it appears that the temperature of the cluster is lower than estimated in Tucker et al. (1998), though it is still one of the hottest known clusters.

The cluster was also observed with the ROSAT HRI in 1995 for 58 ksec (Tucker et al. 1998). A HRI image of the cluster is shown in grey scales in Fig. 3.

2.3. Discussions

The radio halo source in 1E0658-56 is the strongest and largest known at 1.4 GHz. Its flux density of 72.9 ± 0.9 mJy at 1.3 GHz corresponds to a power of $(3.10 \pm 0.04) \times 10^{25}$ W Hz^{-1} within an area ~ 1.2 Mpc^2. The largest linear extent of the halo is ~ 2 Mpc. But this power is likely to be a lower limit since the 1.3 GHz images show clear evidence of missing short spacings: futher ATCA observations with the 210m configuration are needed. The equipartition magnetic field was estimated to be $B_{min} \sim 0.3\mu$G.

The HRI image of the cluster shows that it is a pre-merging system with the two clumps clearly separated. The radio halo has a similar appearance and extent compared with the cluster X-ray emission (see Fig. 3), though less peaked. It is likely that shocks produced through merging have provided the energy necessary for accelerating the radiating electrons. However, the radio halo does not resemble a shock but rather the distribution of thermal electrons that produce the X-rays.

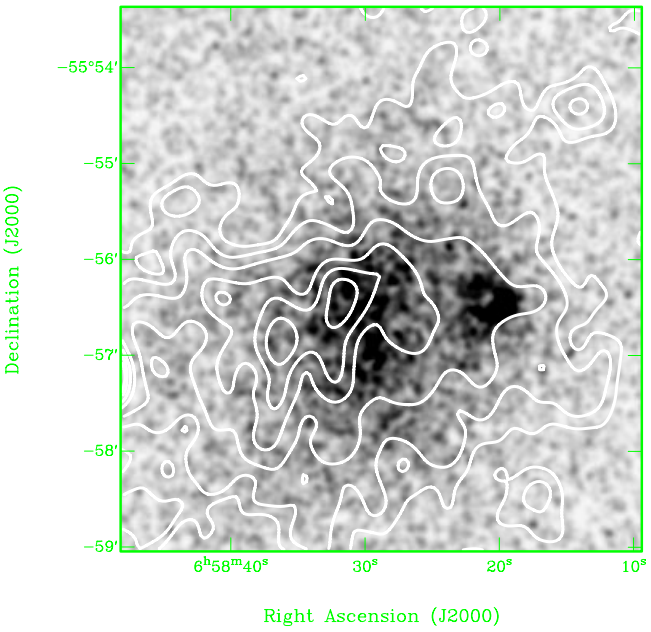

Fig. 3. A contour plot of the radio halo at 1.3 GHz after the subtraction of point sources is overlaid on a ROSAT HRI image smoothed with a Gaussian of $2''$ width. The resolution of the HRI is $\sim 5''$. The radio image is smoothed to a resolution of $\sim 20''$. The contour levels are 0.2, 0.4, 0.8, 1.5, 2.0 & 2.5 mJy/beam. The noise in the image is $\sim 80\mu$Jy/beam.

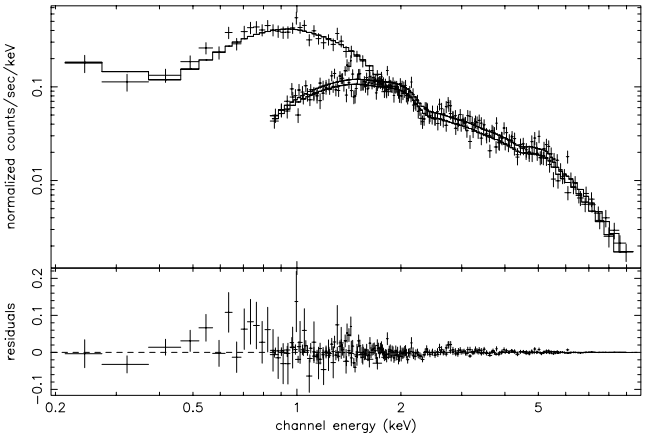

Fig. 4. X-ray spectra from ASCA GIS data and ROSAT PSPC data. A Raymond-Smith thermal spectrum with $kT_x \sim 14.5$ keV after a convolution with instrumental responses is shown as a histogram on the observed spectra (with error bars).

3. The Origin of Radio Halos

3.1. Are radio halos intrinsically rare?

A number of surveys have been conducted to search for radio halos. The earliest were conducted at Green Bank

at 610 MHz (Jaffe and Rudnick 1979), at metre-waves 50-120 MHz (Cane *et al.* 1981) and at Arecibo at 430 MHz (Hanisch 1982), but yielded few examples. Most of the surveys selected either nearby Abell clusters (Hanisch 1982), or clusters with known X-ray emission or radio sources. More recently, Lacy *et al.* (1993) imaged a sample of radio sources from the 8C 38MHz survey (within 3.3° of the North Ecliptic cap) using the Cambridge Low Frequency Synthesis Telescope at 151 MHz but did not find any new halo sources.

Recent X-ray selected surveys of halos as well as observations aimed at detecting the SZ effect have found many more halo candidates suggesting that halos may not be as rare as they were thought to be.

Moffet and Birkinshaw (1989) first suggested that there may be a correlation between the presence of SZ effect and radio halo sources, since the only three clusters A2218, A665 and CL0016+16 which had SZ effect detected at the time also had extended diffuse radio emission. One of the strongest radio halos was found in A2163 in an attempt to detect the SZ effect (Herbig and Birkinshaw 1994). Among the 7 clusters observed at the ATCA for the SZ effect, 3 clusters show clear evidence of a radio halo (A2163, 1E0658-56 & S295), while another 2 clusters showed faint extended emission which can either be the result of the blending of faint discrete radio sources or a faint halo (Liang 1995, Liang et al. 1999). It is perhaps not surprising that searches for the SZ effect have yielded more halo sources than the early surveys since candidates for the SZ effect are hot X-ray luminous clusters. The SZ effect is also cluster-wide, thus diffuse and extended like the halo sources. Any observation designed to search for the SZ effect will optimise the brightness sensitivity and thus favour the detection of halos.

Giovannini et al. (1999) in their correlation of NVSS images with the catalogue of X-ray Brightest Abell clusters (XBAC; Ebeling et al. 1996) found 29 candidate clusters with diffuse radio emissions. They noticed a significant increase in the percentage of diffuse radio sources in high luminosity clusters compared with low luminosity clusters (27-44% in clusters with $L_x > 10^{45}$ ergs/s as compared with 6-9% for $L_x < 10^{45}$ ergs/s).

We conclude that radio halos are not intrinsically rare, and appeared to be rare from the results of early surveys partly because of the difficulty of detecting such low surface brightness objects and partly because of the selection criteria.

3.2. The link between thermal and relativistic electrons

While Giovannini et al. (1999) found an increased occurrence of halos in high X-ray luminosity clusters compared to the low luminosity ones, they did not find a correlation between the radio power of diffuse cluster radio sources and the cluster X-ray luminosity. Instead of plotting radio power against X-ray luminosity, we examine the relationship between halo radio power and cluster X-ray temperature. Fig. 5 shows the 1.4 GHz integrated radio power of cluster halos plotted against the cluster temperature, demonstrating a steep correlation. Only well-confirmed radio halos (not relic sources) are plotted, hence the sample of clusters shown is by no means complete. The apparent rareness of halos can be explained by the steepness of the relationship shown in Fig. 5: only clusters with a high X-ray temperature at moderate redshifts are easily detectable. The surface brightness of halos goes as $(1+z)^{-5}$ when taking account of the K-correction, thus the halo surface brightness rapidly diminishes with increasing redshift. On the other hand, halos with low redshift are also difficult to detect since they tend to be resolved out in simple interferometric maps (or single dish observations without a large beam-throw).

In the 3 well-imaged cluster halos (Coma, A2163 & 1E0658-56), the extent and shape of the radio halo follows closely that of the cluster X-ray emission (Fig. 3; Deiss et al. 1997; Herbig and Birkinshaw 1999). Both the correlation shown in Fig. 5 and the similarities between the radio and X-ray morphology indicate a direct connection between the thermal particles and the relativistic electrons responsible for the radio emission.

3.3. A new model

We propose a new model for radio halos where the thermal electrons in the ICM provide the seed particles for acceleration to relativistic and ultra-relativistic energies necessary for the production of synchrotron emission. This differs from the existing theories (e.g. Jaffe 1977) where the seed electrons diffused out of radio galaxies. In the past, the possibility of the ultra-relativistic electrons originating from thermal electrons accelerated to relativistic energies has been dismissed, usually without much justification. We will examine this issue by looking at the arguments put forward against the possibility of accelerating thermal electrons to relativistic energies. One of the simple arguments was that such a process would be present in every cluster and thus fail to explain the perceived rarity of halos. As discussed earlier, such an argument is rather simplistic: halos may be in every cluster and be detectable or not according to their brightness, which appears to be related to the temperature of the thermal gas.

A second argument against the "thermal pool" origin of the ultra-relativistic electrons was that stochastic processes such as Alfvén, turbulent and shock accelerations are only efficient in accelerating electrons of energy at least several tens of keV (e.g. Eilek & Hughes 1991). This means that either the seed electrons are mildly relativistic already, or an injection process is necessary to create a substantial suprathermal tail in the electron energy distribution. To circumvent the injection process (not yet understood), it is attractive to invoke models that use the

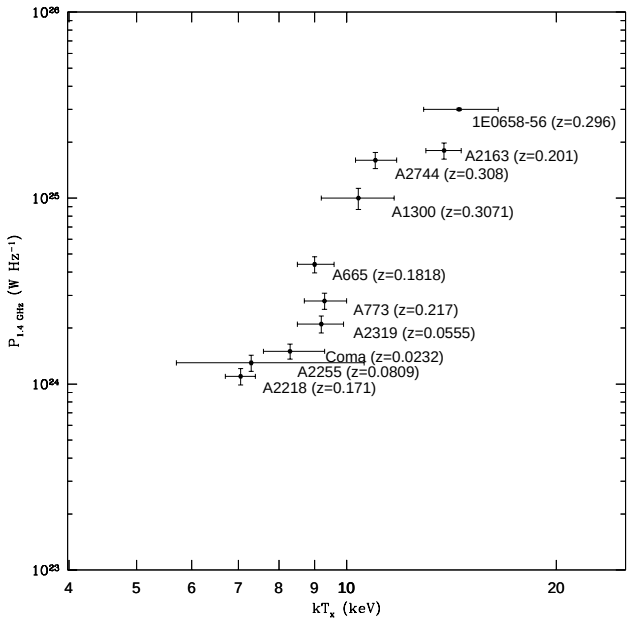

Fig. 5. Radio power $P_{1.4}$ at 1.4 GHz versus the X-ray temperature kT_x for cluster-wide radio halo sources. The error bars for the intracluster gas temperature correspond to a 90% confidence limit. Formal errors of $\sim 1\sigma$ are given for the halo power where it is known, in cases where the errors are not obviously stated in the literature, a 10% error is assumed. The data are obtained from Reid et al. 1999, Pierre et al. 1999, Herbig & Birkinshaw 1999, Allen & Fabian 1998, Mushotzky & Scharf 1997, Giovannini et al. 1999, Feretti et al 1997, Giovannini et al. 1993, Markevitch et al. 1998, David et al. 1993 and Ferretti *et al.* this proceedings. The highest flux density is taken, where a halo has been observed more than once at 1.4 GHz.

already-relativistic electrons from radio galaxies as seed particles to be re-accelerated.

However, observationally, it has also been shown that while halo candidates were found in nearly 30% of the high X-ray luminosity clusters in a survey for radio halo sources, none was found in the 19 clusters selected by their over-abundance of tailed radio sources (Giovannini et al. this proceedings). This is further evidence that the relativistic electrons are more likely to have originated from the thermal pool of electrons than the radio galaxies: the appearance of halos is more closely linked to thermal X-ray emission than the presence of tailed radio galaxies.

A closer examination of the argument for an injection process show that it may not always be necessary in a cluster environment. According to Eilek & Hughes (1991), electrons need a minimum energy to be accelerated by Alfvén waves. In low density environments, this minimum energy is already mildly relativistic. However, in a high density environment, where $n_e > 10^{-3} B_{\mu G}^2\,\mathrm{cm}^{-3}$, an electron can resonate with Alfvén waves at sub-relativistic energies of $\frac{1}{2} m_p v_A^2 / \cos^2\theta$ (where v_A is the Alfvén speed and θ is the pitch angle), i.e. energies of a few eV. The environments of radio galaxies, including clusters, were considered to be of low density since the magnetic field strength B was thought to be a few μG, which means the density threshold is much higher than most cluster environments. Recent hard X-ray results from Beppo-SAX and Rossi-RXTE for Coma and other clusters have shown the magnetic field to be $B \sim 0.2\mu$G if the excess hard X-ray emission is due to inverse Compton scattering of relativistic electrons by the CMB (e.g. Fusco-Femiano et al. 1999; Rephaeli et al. 1999; Valinia et al. 1999). Thus the density threshold is now $\sim 4 \times 10^{-5}\,\mathrm{cm}^{-3}$, which makes most parts of clusters high density environments. Therefore, it is possible to accelerate thermal electrons in clusters through resonance with Alfvén waves, and in the mean time, Dogiel (this proceeding) has shown that it is possible to produce a substantial suprathermal tail in the electron energy distribution through second order Fermi acceleration in cluster environments.

Both merging activity and the thermal electron temperature maybe responsible for the production of radio halos. A possible scenario would be that the initial merging activity provides the energy for accelerating electrons from the suprathermal tail of the energy distribution (where the hotter clusters have more power) to ultra-relativistic energies. After the shocks have disappeared, radio halos like that of 1E0658-56 may be maintained by in-situ electron acceleration in the residual turbulence.

Cooling flow clusters are thought to be relaxed and devoid of merging activities. Most of the clusters shown in Fig. 5 are non-cooling flow clusters. This does not imply that mergers are the *critical* element in radio halo formation, since it could be the result of selection effects: cooling flow clusters are more likely to have a significant central radio source than a non-cooling flow cluster (e.g. Peres et al. 1998). To our knowledge, no cluster with a strong cooling flow has been observed properly to be able to test whether or not it follows the $P_{1.4}-kT_x$ trend shown in Fig. 5. To illustrate the need for proper observations with high brightness sensitivities, we give as an example, RXJ1347-11, a strong cooling flow with a very high gas temperature of $\sim 12.5\,\mathrm{keV}$ (Allen and Fabian 1998) which has been observed by the NVSS with no obvious detections. However, the NVSS does not have enough brightness sensitivity to detect, in RXJ1347-11, a halo similar to that in 1E0658-56 because of the high redshift ($z \sim 0.45$) of the cluster and the high noise levels in the NVSS image ($\sim 0.5\,\mathrm{mJy}$ per $45''$ beam).

4. Conclusions

We have found a strong radio halo source in the cluster 1E0658-56. At a 1.3 GHz radio power of $(3.1 \pm 0.1) \times 10^{25}\,\mathrm{W\,Hz^{-1}}$, it is one of the most powerful radio halo sources. It has a steep spectral index of $\alpha_{4864}^{1344} \sim -1.2$ typical of known halos. The brightness distributions of the radio halo and X-ray emission from the cluster gas are

remarkably similar, suggesting a direct relationship between the ultra-relativistic electrons responsible for the synchrotron emission and the thermal intracluster gas. As further evidence for the radio/X-ray connection, we have found a steep correlation between the radio power of the halo and the X-ray temperature of the intracluster gas ($P_{1.4}$ vs kT_x) from the 10 confirmed cluster radio halos. We suggest a new explanation for the origin of radio halo sources, where the high energy tail of the thermal electron distribution is boosted to ultra-relativistic energies, thus providing a natural link between the halo radio power and X-ray gas temperature. Finally, it is important for our understanding of the origin of radio halo sources to establish the robustness of the $P_{1.4} - kT_x$ correlation by observing a temperature selected sample of clusters, and to test the mechanism by searching for halos in clusters with strong cooling flows but high temperature.

Acknowledgements. I would like to thank Sarah Maddison for help with the ATCA observations. It is a pleasure to acknowledge the input from my collaborators Mark Birkinshaw, Paola Andreani and Richard Hunstead, as well as discussions with and encouragements from other conference participants, especially R. D. Ekers, J. Eilek, V. Dogiel and A. Edge. The Australia Telescope is funded by the Commonwealth of Australia for operation as a National Facility managed by CSIRO.

References

Allen S. & Fabian A., 1998, MNRAS 297, 57
Andreani P., Böhringer H., Dall'Oglio G., Martinis L., Shaver P., Lemke R., Nyman L., Booth R., Pizzo L., Whyborn N., Tanaka Y. & Liang H., 1999, ApJ 513, 23
Cane H., Erickson W., Hanisch R. & Turner P., 1981, MNRAS 196, 409
David L., Slyz A., Jones C., Forman W., Vrtilek S. & Arnaud K., 1993, ApJ 412, 479
Deiss B., Reich W., Lesch H. & Wielebinski R., 1997, A& A 321, 55
Dennison B., 1980, ApJ 239, L93
Ebeling H., Voges W., Böhringer H., Edge A., Huchra J. & Briel U., 1996, MNRAS 283, 1103
Eilek J. & Hughes P., 1991, in "Beams and Jets in Astrophysics", Cambridge Astrophysics Series.
Feretti L. & Giovannini G., 1996, in IAU symposium 175, "Extragalactic radio sources".
Feretti L., Giovannini G. & Böhringer H., 1997, New Astronomy 2, 501
Feretti L., Böhringer H., Giovannini G. & Neumann D., 1997, A& A 317, 432
Fusco-Femiano R., et al., 1999, astro-ph/9901018
Giovannini et al., 1999, astro-ph/9904210
Hanisch R. J., 1982, A&A 111, 97
Harris D. E., Kapahi V. K., & Ekers R. D., 1980, A& A Suppl., 39, 215
Herbig T. & Birkinshaw M., 1994, AAS 185, 3307
Herbig T. & Birkinshaw M., 1999, in preparation
Jaffe W., 1977, ApJ 212, 1
Jaffe W. & Rudnick L., 1979, ApJ 233, 453
Lacy M., Hill G., Kaiser M. & Rawlings S., 1993, MNRAS 263, 707
Liang H., 1995, Thesis, ANU
Liang H., Hook I., Shaver P., Ekers R.D., Böhringer H., Andreani P., 1999, in preparation
Markevitch M., Forman W., Sarazin C. & Vikhlinin A., 1998, ApJ 503, 77
Moffet A. & Birkinshaw M., 1989, AJ 98, 1148
Morrison R. & McCammon D., 1983, ApJ, 270, 119
Mushotzky R. & Scarf C., 1997, ApJ 482, L13
Peres C., Fabian A., Edge A., Allen S., Johnston R. & White D., 1998, MNRAS 298, 416
Pierre M., Matsumoto H., Tsuru T., Ebeling H. & Hunstead H., 1999, A& A suppl. 136, 173
Raymond, J. C.,& Smith, B. W., 1977, ApJs, 35, 419
Reid A., Hunstead R., Lémonon L. & Pierre M., 1999, MNRAS 302, 571
Rephaeli Y., Gruber D., & Blanco P., 1999, ApJ 511, L21
Roland J, 1981, A&A 93, 407
Röttgering H., Wieringa M., Hunstead R. & Ekers R., 1997, MNRAS 290, 577
Sunyaev, R. A., & Zel'dovich Ya.B., 1972, Comm. Astr. Spa. Phys. 4. 173
Tucker W. H., Tananbaum H., Remillard A. A., 1995, ApJ 444, 532
Tucker W. H., Blanco P., Rappoport S., David L., Fabricant D., Falco E.E.,Forman W., Dressler A., Ramella M., 1998, ApJ 496, L5
Tribble P., 1993, MNRAS 263, 31
Valina A. et al., 1998, astro-ph/9812477

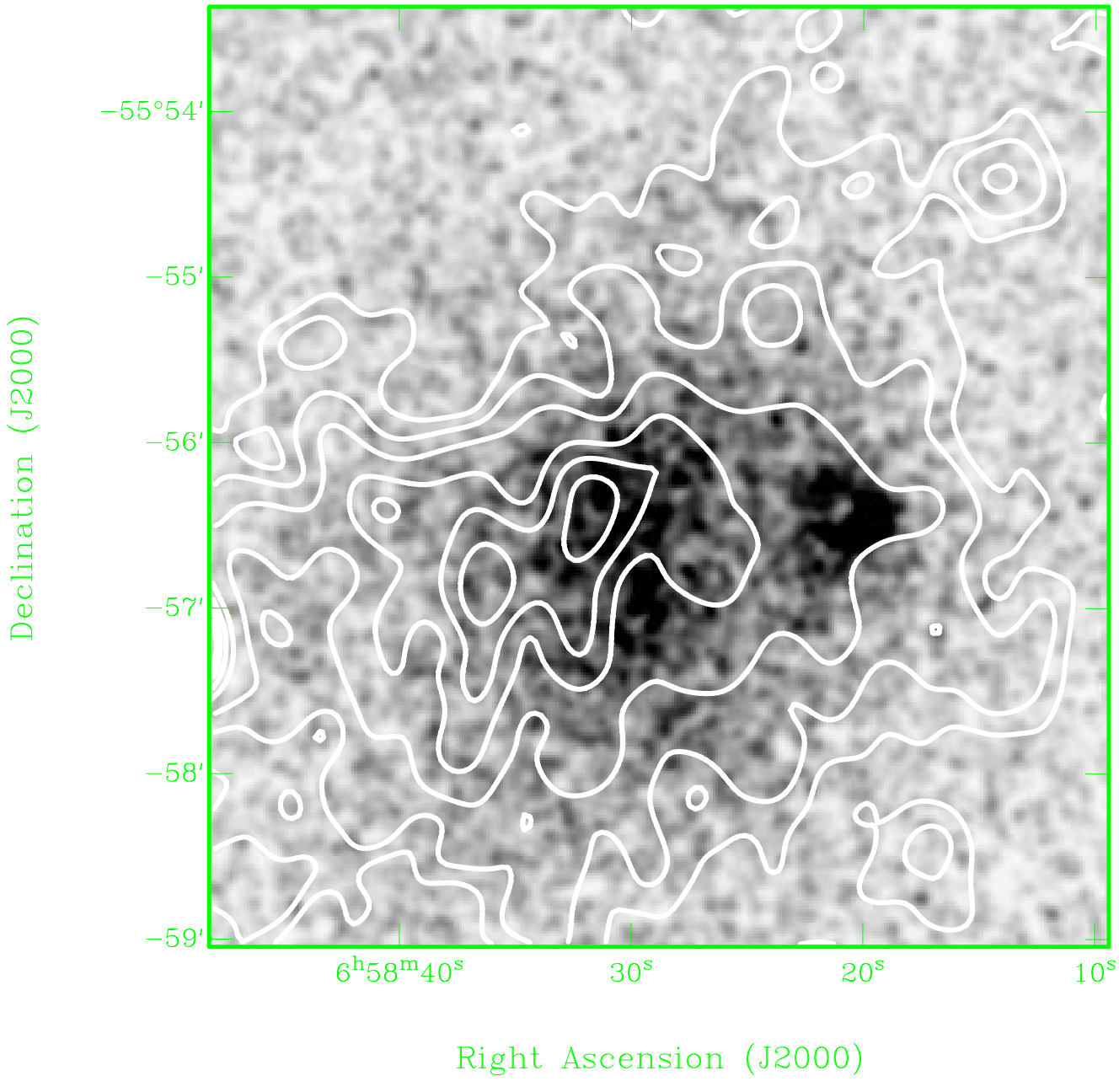
−55°54′
−55′
−56′
−57′
−58′
−59′
Declination (J2000)
6h58m40s
30s
20s
10s
Right Ascension (J2000)